Numerical Analysis of Interaction between Moving Shock Wave and Solid Particle Layer

K. Doi and Y. Nakamura

1 Introduction

When a shock wave propagates over many small solid particles on a horizontal wall, some particles near the surface of the layer are lifted and dispersed into the shock-induced flow. These dispersed particles is called the dust cloud. This phenomenon is actually seen in galleries of coal mines or in pipelines for neumatic transportation of powder, and mixing dispersed flammable dust particles with high-temprature and high-pressure gas behind the shock wave sometimes causes the dust explosion. And this phenomenon includes some interesting factors, such as the shock structures interacted with the dust layer, interactions between gas and solid particle, and interactions between solid particles.

This phenomenon has been investigated by many researchers. Dawes[1] reproduced the dust cloud by the shock-tube experiment, and examined the characteristics. Gerrard[2] and Fletcher[3] conducted similar shock-tube experiments to examine the initial stage of the dust cloud formation, but the dyanmical mechanism was not able to be shown clearly. Bracht[4] searched for the transitional regime to turbulent flow in the dust cloud by the observation of more time. Suzuki et al.[5] examined the translational and rotational motions of dust particles in detail. On the other hand, Khul et al.[6] conducted the numerical simulation based on the mixture model, and showed appearance of a vortex generated from the interaction between the shock wave and dust layer by baloclinic effect. Jiang[7] and Thevand[8] also conducted the numerical simulation based on the two fluid model. However, they has not shown the dynamic structure of the dust cloud formation clearly.

In the present study, it aims to pay attention at the initial stage of the dust cloud formation process, and to clarify the dynamic mechanism by the numerical simulation. A discrete model is applied to the solid particles whereas a continuum model is applied to the gas in this simulation. As a result, the dynamic status of an individual

K. Doi · Y. Nakamura
Department of Aerospace Engineering, Nagoya University Furo-cho,
Chikusa-ku, Nagoya, 464-8603 Japan

particle that composes the dust cloud can be clearly shown, and the particle-particle interaction can be considered easily in addition.

2 Computational Model

Governing equations for gas phase are as follows.

$$\frac{\partial}{\partial t}(m_f) + \nabla \cdot (m_f \mathbf{u}_f) = 0 \tag{1}$$

$$\frac{\partial}{\partial t}(m_f \mathbf{u}_f) + \nabla \cdot (m_f \mathbf{u}_f \mathbf{u}_f) = -\alpha_f \nabla p + \alpha_f \nabla \cdot \mathbf{T} - \mathbf{F}_i \tag{2}$$

$$\begin{aligned} \frac{\partial}{\partial t}(m_f E_f) + \nabla \cdot (m_f H_f \mathbf{u}_f) \\ = \nabla \cdot (\alpha_f \mathbf{T} \cdot \mathbf{u}_f) - \nabla \cdot (\alpha_f \mathbf{q}) - Q_i \end{aligned} \tag{3}$$

$$p = \rho_f R T_f \tag{4}$$

$\rho_f, p, \mathbf{u}_f, T_f, E_f, H_f$ is gas density, pressure, velocity vector, temperature, total energy, and total entalpy, respectively. α_f is void fraction, and $m_f = \alpha_f \rho_f$. R is gas constant. $\mathbf{T}$ is gas viscous tensor, and $\mathbf{q}$ is gas heat conduction. $\mathbf{F}_i$ and Q_i are interactions of momentum and energy between gas and solid particles.

Governing equations for each solid particle are as follows.

$$\frac{d}{dt}(\mathbf{r}_p) = \mathbf{u}_p \tag{5}$$

$$\frac{d}{dt}(m_p \mathbf{u}_p) = \mathbf{f}_i + \mathbf{f}_c + m_p \mathbf{g} \tag{6}$$

$$\frac{d}{dt}(I_p \omega_p) = \mathbf{M}_i + \mathbf{M}_c \tag{7}$$

$$\frac{d}{dt}(C_p T_p) = q_i + q_c \tag{8}$$

$\mathbf{r}_p, \mathbf{u}_p, \omega_p, T_p$ is position, translational velocity, rotational velocity, and temperature of the particle, respectively. m_p, I_p, C_p is mass, moment of inertia, and heat capacity of the particle, respectively. $\mathbf{f}_i$,$\mathbf{M}_i$, and q_i are interactions of momentum, angular momentum, and energy between gas and each particle. $\mathbf{f}_c$, $\mathbf{M}_c$, and q_c are particle-particle and particle-wall interactions.

The gas-particles interactions, $\mathbf{f}_i$, $\mathbf{M}_i$, and q_i, are assumed to be composed of drag force, $\mathbf{f}_{iD}$, Saffman force, $\mathbf{f}_{iS}$, Magnus force, $\mathbf{f}_{iM}$, macroscopic pressure gradient,

$\mathbf{f}_{iP}$, drag torque $\mathbf{M}_{iD}$, and heat transfer q_{iT}. They are estimated by some results of experimental measurements and numerical simulations for a sphere.

The particle-particle and particle-wall interactions, $\mathbf{f}_c$ and $\mathbf{M}_c$, are estimated by the discrete element model (DEM), where elastic collisions are modeled by springs, dampers, and sliders.

3 Computational Method and Conditions

The governing equations for gas phase are discretised in space by the finite volume method. The solution vectors at the cell-boundary are evaluated by the 3rd order MUSCL method with Van Albada's limiting function, and then the invicid flux is estimated by the approximated Riemann solver. And, spatial gradients of solution vector is estimated by the least square method. On the time integrations, LU-SGS method is used for the gas-phase and the two-stages Runge-Kutta method for solid particles, and they are coupled weakly.

The gas phase is air, and the viscous coefficient is estimated by the Sutherland's equation. The shock wave Mach number is $M_S = 1.44$. The shock-induced flow velocity is $U_O = 211[m/s]$ and the particle Reynolds number is $Re_D = 2100$ in this condition. Each solid particle is a sphere, the diameter is $D = 0.1[mm]$Cthe density is $\rho_p = 980[kg/m^3]$, and the heat capacity is $c_p = 1200[J/kgK]$. As parameters of the DEM, the spring coefficient is $k = 2.05 \times 10^4[N/m]$, the damper coefficient is $c = 7.33 \times 10^{-4}[Ns/m]$Cand the Coulomb's friction coefficient is $\mu = 0.3$, the restitutive coefficient at the collision is $e = 0.7$ and the contacting period is $T_c = 0.5[\mu s]$ in these conditions.

The computational domain is three-dimensional, $0 \leq x \leq 400[mm]$, $0 \leq y \leq 0.3[mm]$, $0 \leq z \leq 100[mm]$. And a trough with depth of $2[mm]$ on the wall of $100 \leq x \leq 400[mm]$ is set to accumurate the solid particles. The conditions of the solid particle layer are shown in Table 1.

Table 1 Conditions of particle size and initial distributions of solid particle layer.

	DL1	DL2	DL3
Basic diameter D [mm]	0.10	0.10	0.10
Contact diameter D_c [mm]	0.10	0.14	0.10
Number of particles N_p	202,000	104,000	101,000
Mean volume fraction $\overline{\alpha_p}$	0.59	0.30	0.29
Particle contact condition	Contact	Contact	Dispersed

4 Results and Discussions

Distribution of solid volume fraction and gas pressure at $t = 0.8[ms]$ in the case of DL1 are shown in Figure 1(a), Figure 1(b), respectively. The shock wave propagated from left to right, the shock is at the position of 290[mm] from a leading edge of the dust layer. The dust cloud is formed behind the shock, where the pressure is disturbed.

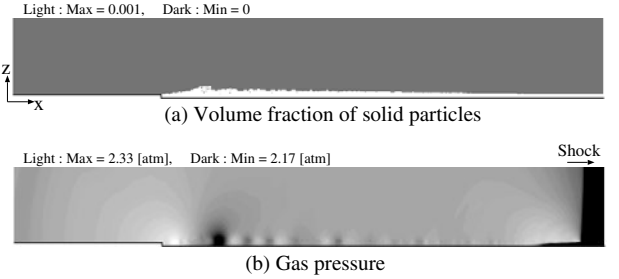

(a) Volume fraction of solid particles

(b) Gas pressure

Fig. 1 Shock wave propagating on the solid particle layer in the case of DL1.

The distributions of solid particles composing the dust cloud at $t = 0.8[ms]$ is shown in Figure 2. The horizontal axis is the distance from the shock, X, and the vertical axis is the height from the surface of the dust layer, h. Comparing the height of computational result with the experimental result, they are almost corresponding. And, it can validate the computational results in this study.

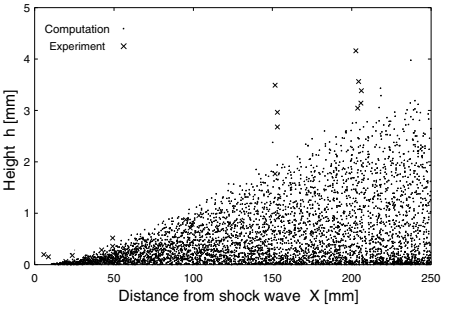

Fig. 2 Distribution of solid particles composing the dust cloud in the case of DL1, The "computation" means the height of each particle in the computational result of this study, the "experiments" means the maximum height of particles in the experimental results conducted by Suzuki et al.[5].

Outer shapes of the dust clouds in each cases of initial solid particle layer, DL1, DL2, and DL3 are shown in Figure 3. And, one in the case of DL1 without Saffman and Magnus forces are also shown in the same figure. It is shown in this figure that the initial condition of the solid particle layer, contacted (DL1,DL2) or dispersed(DL3), is more dependent on the height of the dust cloud than the fluid lift forces. This result means that dust cloud formation is mainly caused by particle-particle direct interactons, that is contacts and collision between solid particles at the initial stage of the dust cloud formation.

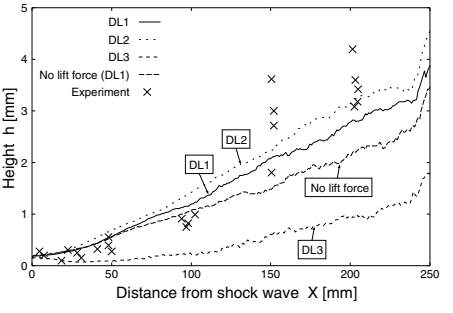

Fig. 3 Outer shapes of dust clouds; effects of initial condition of the solid particle layer and fluid lift force

Pressure distribution where the shock wave interacts with the solid particle layer in the case of DL1 and DL2 are shown in Figure 4. It is shown that the shock wave on the surface of the solid particle layer is curved by the interaction, and it raises the pressure on the surface behind the shock. And, the interaction in the case of DL2, higher void fraction, is stronger than that in the case of DL1, lower void fraction.

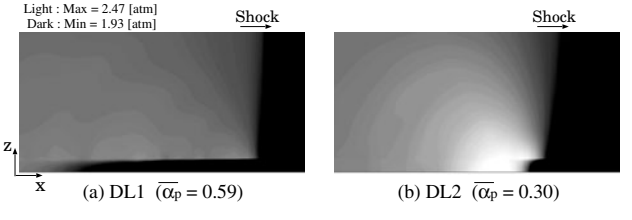

Fig. 4 Gas pressure distributions in shock structures interacting with dust layer; effect of the void fraction of the solid particle layer

Distributions of gas pressure and particle-contacting pressure on the bottom wall of the solid particle layer are shown in Figure 5. The gas pressure in this figure is a difference from that in front of the shock wave, and the particle-contacting pressure is averaged over 1[mm]. Furthermore, both of pressure values are nondimensionalized by the difference between the pressure behind the shock and that in front of the

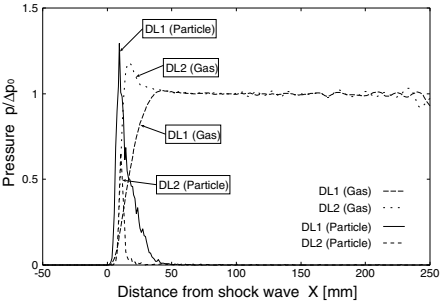

Fig. 5 Gas and solid particles pressure distributions on wall in overpressure behind shock

shock. The curvature of the shock generates the downward flow behind the shock, and then the downward flow pressed the solid particles to the bottom wall and raises the gas pressure in the solid particle layer behind the shock.

5 Conclusion

In the present study, the initial process of forming the dust cloud was numerically simulated to examine its dynamic mechanism. The simulated dust cloud was close to experimental results. It was found by comparing several types of dust layers that the upward velocity of lifted particles was more produced by particle-particle interactions than by fluid lift forces such as the Saffman force and the Magnus force. Moreover, it was confirmed that a relatively strong downward flow was induced just behind the foot of the shock by its curved shape, which promotes the interactions and causes an overpressure on the wall.

References

1. Dawes, J.G.: Safety in Mines Research Establishment, vol. 36, pp. 1–69. Ministry of Fuel and Power, England (1952)
2. Gerrard, J.H.: Brit. J. Appl. Phys. 14, 186–192 (1963)
3. Fletcher, B.: J. Phys. D: Appl. Phys. 9, 197–202 (1976)
4. Bracht, K., Merzkirch, W.: Int. J. Multiphase Flow 5, 301–312 (1979)
5. Suzuki, T., Adachi, T.: JSME Journal B 52, 483, 3742–3746 (1986)
6. Khul, A.L., Ferguson, R.E., Chien, K.Y., Collins, P.: Progress in Astronautics and Aeronautics, vol. 154, pp. 491–515. AIAA, Wash., D.C. (1993)
7. Jiang, J.P.: Ph. D. Dissertation of Ben-Gurion University of the Negev (1996)
8. Thevand, N., Daniel, E.: Shock Wave 11, 279–288 (2002)